CLOUD ATTENUATION AT Ka, Q AND W BANDS BASED ON RADIOSOUNDINGS DURING RAINY AND NON-RAINY SEASONS IN CENTRAL ANDES: A STUDY IN EL ALTO, BOLIVIA

ATENUACIÓN POR NUBES EN BANDA Ka, Q Y W EN BASE A RADIOSONDEOS DURANTE TEMPORADAS DE LLUVIA Y SECA EN LOS ANDES CENTRALES: ESTUDIO EN EL ALTO, BOLIVIA

Alejandro Garcia, Gustavo Siles, Juan Pablo Arciénega and Yasmin Balderrama

Laboratorio de Radiocomunicaciones (LRC)

Universidad Privada Boliviana

gustavosiles@upb.edu

ABSTRACT

Cloud attenuation in satellite communication systems becomes a relevant issue as the frequency increases, and thus, it has to be taken into account when link availability is being calculated. This atmospheric impairment is a variable atmospheric phenomenon whose characterization has to be done not only on a yearly-basis but also on a seasonal and monthly basis. In the present paper, cloud attenuation statistics are reported at 20 GHz, 40 GHz and 75 GHz during rainy and non-rainy seasons in El Alto, Bolivia, at 4065 m of altitude, using 3 years of radiosoundings (2016-2019). Cloud detection models have been used for the calculations, including Salonen, Salonen08, Decker and CldMod models, and results obtained are compared to those given by the global model of the ITU-R Rec. P.840. The results lead to conclude that zenith cloud attenuation during rainy season can reach maximum values between 0.15 and 0.45 dB (20 GHz), 0.55 and 1.5 dB (40 GHz), and 1.3 and 3.9 dB (75 GHz) depending on the model to be used. In comparison, during non-rainy season these values vary between 0.08 and 0.33 dB (20 GHz), 0.26 and 1.1 dB (40 GHz), and 0.62 and 2.6 dB (75 GHz). On the other hand, statistics based on CldMod model and, in a less extent, Decker model are close to the ones obtained using the ITU-R global model. These observations could open the possibility of further studies assessing the reliability of meteorological parameters in digital maps at high altitude sites, because these data are used in global propagation models.

Keywords: Satellite Communications, Cloud Attenuation, Propagation, Radiosoundings.

RESUMEN

La atenuación por nubes en sistemas de comunicaciones por satélite adquiere mayor importancia a medida que aumenta la frecuencia de operación del sistema. Se trata de un fenómeno variable cuya caracterización es imprescindible, no sólo sobre una base estadística anual sino también estacional. En este artículo se presentan estadísticas de atenuación por nubes en 20 GHz, 40 GHz y 75 GHz durante los periodos de lluvia y no-lluvia a 4065 m de altitud, basados en el análisis de 3 años de radiosondeos (2016-2019) en El Alto, Bolivia. Se utilizan los modelos de Salonen, Salonen08, Decker y CldMod y los resultados se comparan con el modelo global de la Rec. UIT-R P.840. Los resultados llevan a concluir que la atenuación cenital debida a nubes durante época de lluvia puede alcanzar valores máximos entre 0.16 y 0.45 dB (20 GHz), entre 0.5 y 1.5 dB (40 GHz), y entre 1.3 y 3.9 dB (75 GHz) dependiendo del modelo que fue utilizado. En comparación, durante época de no-lluvia estos valores varían entre 0.08 y 0.33 dB (20 GHz), entre 0.26 y 1.1 dB (40 GHz), y entre 0.62 y 2.6 dB (75 GHz). Por otro lado, las estadísticas en base a los modelos CldMod y, en menor medida, Decker se aproximan mejor a los resultados del modelo de la UIT-R. Estas observaciones abren la posibilidad a trabajos adicionales que evalúen la confiabilidad de los parámetros meteorológicos de los mapas digitales modelos globales en sitios con una altitud considerable, debido a que éstos se utilizan en modelos de propagación globales.

Palabras Clave: Comunicaciones Satelitales, Atenuación Por Nubes, Propagación, Radiosondeos.

1. INTRODUCTION

The increasing demand of bandwidth by end users of satellite communication systems, which are suitable to reach those regions without neither fiber nor cellular coverage, is moving operators to use high frequencies. However, as a well-known rule of thumb, as frequency increases the propagation impairments become more critical, negatively affecting the availability of satellite links, thus the QoS (Quality of Service) offered by operators. To date, most of propagation studies found in the technical literature have been developed in the Northern hemisphere and temperate regions. In recent years, also tropical climates have drawn attention from propagation scientific community. However, to our knowledge, high altitude regions where weather conditions would be at the origin of better propagation conditions have not been studied yet. In this sense, the Propagation Series (P-series) of the ITU-R (International Telecommunications Union, Radiocommunication sector) Recommendations should be assessed in such conditions because some countries,

including Bolivia, have population living in isolated communities in Andean regions, where altitude can be as high as 4000 meters a.m.s.l.

TABLE 1 - GENERAL CHARACTERISTICS OF RADIOSONDE

Site	El Alto Airport
Period	08/2016 to 07/2019
Launch time	12:00 UTC
Radiosonde model	Vaisala RS92-SGP
File format	TSV (Tab Separate Value)
Vertical resolution (m)	10-15
Time elapsed between vertical levels (s)	2
Number of valid radiosondes	722

Figure 1: Location of the radiosonde launching site at the El Alto Airport, in La Paz city, Bolivia.

The present work is focused on the estimation of cloud attenuation at Ka-band, currently used for high data rate satellite connectivity, and also at Q- and W-bands, as they have been announced as candidate frequencies for future SatCom systems [1][2]. In particular, the aim of this work is the estimation of statistics of cloud attenuation during rainy and non-rainy seasons at a high altitude site, therefore extending the previous results reported in [3]. For this purpose, a multi-year database of radiosoundings carried out in El Alto Airport (La Paz, Bolivia) has been analyzed. The vertical meteorological profiles extracted from these measurements are used as input data of models allowing the presence of clouds to be detected and their water liquid content to be estimated. Cloud attenuation statistics obtained using these models, both in rainy and non-rainy seasons, have been then compared with similar statistics computed using the well accepted ITU-R global model given in the last version of the P.840 Recommendation [4], which is the main reference for satellite communication link designers.

The remainder of the present paper is organized as follows. After this brief introduction, Section 2 describes the geographical site and its mean precipitation characteristics allowing to identify rainy and non-rainy seasons. The methodology used for processing the input data is described in Section 3. The models to detect de presence of clouds and the methods used to calculate cloud attenuation are summarized in Section 4. The main results are presented in Section 5 in the form of seasonal statistics of cloud attenuation at the frequencies of interest, and main conclusions are drawn in Section 6.

2. SITE DESCRIPTION

The Bolivian National Service of Meteorology (SENAMHI) provided 3 years of vertical meteorological profiles used in this work. These data were collected from August 2016 to July 2019, in El Alto Airport, located in La Paz city, Bolivia (see Figure 2). This station is located at 16.51° S, 68.17° W at an altitude of 4065 meters above mean sea level. In total, the database is composed of 733 radiosondes, launched at 12:00 UTC, during working days. Table I provides further technical information on the dataset.

TABLE 2 – HISTORICAL AVERAGE PRECIPITATION DATA 1981-2000 IN EL ALTO AIRPORT DATA EXTRACTED FROM [5]

Month	Accumulated precipitation (mm)	Percentage of rainy days (%)
January	135.3	70
February	94.8	63
March	83.2	52
April	35.5	35
May	10.6	12
June	8.4	9
July	6.7	7
August	13.9	14
September	28.4	26
October	46.0	37
November	54.6	42
December	91.6	55

El Alto is located in the Central Andes, a high altitude mountainous territory extended between the western side of Bolivia and southeast region of Peru, with an average altitude of 3700 m.a.s.l. A 30-year exhaustive study performed by Andrade et. al. [5] shows that extreme climate events can occur in this region because it represents "a formidable obstacle to the tropospheric circulation", i.e. a massive geographical barrier between ocean and low altitude continental regions. Between these events, precipitations occur in well differentiated periods of the year, as it can be seen in Table 2, where rainfall data corresponding to El Alto Airport are shown. Between May and August, accumulated rain is small in comparison to that observed between November and February. In particular, January is the month with the highest percentage of rainy days, i.e. days where precipitation is observed. As it is pointed out in [5], April can be considered as a transition month between rainy and non-rainy seasons, and, in the opposite way, October and November represent a change from non-rainy to rainy seasons. Following this observations, for the purpose of this study, wet and dry seasons have been identified in the following way:

- Rainy (wet) season: November to March
- Non-rainy (dry) season: April to October

3. DATA PROCESSING METHODOLOGY

SENAMHI distributes radiosoundings by free to authorized users, including universities, research centers and governmental offices. Quality check (QC) of the data was performed with the aim of discarding invalid vertical meteorological profiles. According to the QC procedure implemented, radiosondes were flagged as non-useful if one of the following criteria was verified:

- Incorrect temperature data.
- Incorrect pressure data.
- Incorrect relative humidity data.
- Equal height levels.
- Heights reach an altitude below 15000 meters.

After identifying and discarding non-useful radiosoundings, about 98.5 % of them have been considered as valid, i.e. a total of 722 radiosoundings. A valuable characteristic of these meteorological profiles launched at El Alto Airport is their vertical resolution, ranging between 10 – 15 meters, which provides a good physical description of the atmospheric path. However, unfortunately, the presence of rain during radiosonde launchings was not assessed because data from on-site rain detection instruments were not available. Therefore, it is likely that some vertical profiles might correspond to instants where rainfall occurred, which could affect in a certain way our results. This fact is well-known in propagation studies and it is normally assumed that a radiosounding under the presence of rain happens with a very low probability.

Data processing routines were implemented in order to estimate Integrated Liquid Water Content, L in mm, for each profile. This physical parameter describes the total amount of cloud liquid water. It keeps a straight relation with attenuation caused by clouds, A_c in dB, as seen in the method described in Section 3.2 of the ITU-R P.840 [4]. This method uses local data, either in the form of point measurements, e.g. using a multi-frequency radiometer, or estimations from vertical meteorological profiles. This procedure to estimate A_c is iteratively repeated for all valid radiosoundings. This general procedure is outlined in Figure 2.
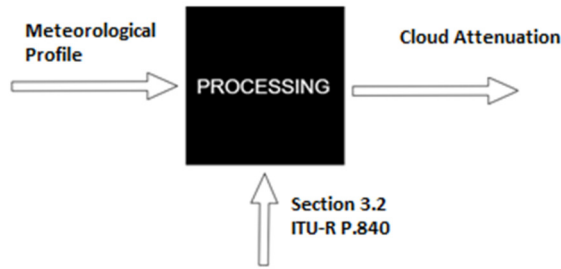
Figure 2: General description of the procedure for obtaining cloud attenuation, combining the estimate of *L* from radiosoundings and the ITU-R P.840 method based on *L* data.

Figure 3 shows a more detailed description of the procedure above described. Once a radiosounding is flagged as valid, vertical interpolation is carried out in order to obtain atmospheric pressure, *P* in hPa, and relative humidity, *RH*, profiles with uniform number of layers of 10-m thickness. Both profiles are used to calculate the critical humidity or threshold function, U_c for every radiosounding. Different functions, summarized in Section 3, are proposed in the Decker, Salonen and Salonen08 models. The presence of a cloud layer along the atmospheric path is detected in those 10-m layers where *RH* is higher than the corresponding U_c threshold. An example of this detection procedure, corresponding to a radiosonde launched in February 2nd, 2018, is shown in Figure 4 where a *RH* profile and U_C functions are plotted. As it can be seen, the detection thresholds can notably vary one from each other, so the vertical structure of a detected cloud will be also quite different from one model to another. Finally, the liquid water content, w_l in g/m^3, of each layer is calculated using expressions provided in the models and the value of *L* is obtained by vertical linear interpolation.
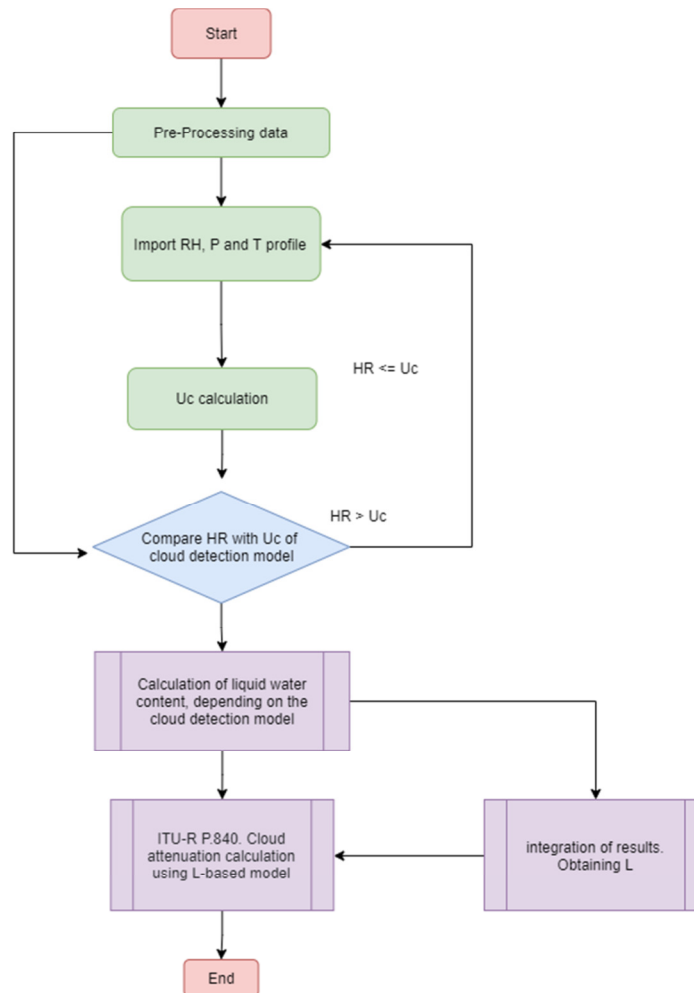.

Figure 3: Flow diagram of the algorithm used for detecting the presence of cloud layers and estimating cloud attenuation from vertical meteorological profiles in combination with cloud detection models.
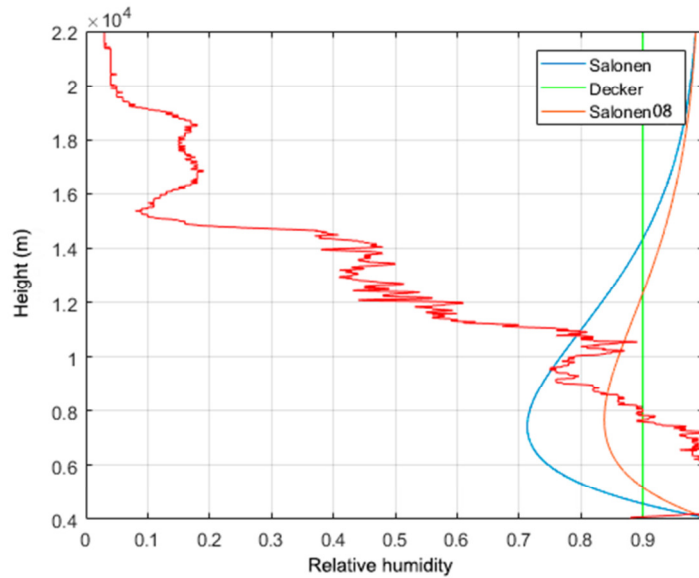
Figure 4: Comparison between Decker, Salonen and Salonen08 relative humidity thresholds
RH profiles corresponding to El Alto (La Paz), February 2nd, 2018, 12:00 UTC.

4. CLOUD DETECTION AND CLOUD ATTENUATION MODELS

4.1. Empirical methods of cloud detection and estimation of liquid water content

Several models for detecting clouds and calculating the amount of liquid water content and ice water content, w_i in g/m^3, into a cloud have been proposed in the technical literature. Among them, some has been extensively used in satellite propagation studies, i.e. the Salonen model. Below, a brief description of the models implemented in the present work. References to the original papers with further details are included for the interested reader.

- Salonen model: Developed by Salonen and Uppala [6] and also known as the Teknillinen KorkeaKoulu (TKK) model, it was tested in several sites located in Europe. The relative humidity threshold U_c at each atmospheric layer depends on the ratio between its atmospheric pressure and that at surface level. Once a cloud layer is detected w_l is estimated using as input data the cloud base height and the *T* profile.
- Salonen08 model: This model was developed by Mattioli et. al. [7] using data from meteorological instruments from the Atmospheric Radiation Measurement (ARM) Program's Southern Great Plaints (SGP) in US. It proposes a new set of parameters for the expressions given by Salonen in [6] for the calculation of both U_c and w_l. This set was the result of a tuning procedure using a laser ceilometer for accurate detection of the presence of clouds.
- CldMod model: Also proposed by Mattioli, et. al. in [7], this model uses the function U_c given by the Salonen08 model, but develops a new expression for calculating the value of w_l in each cloud layer. In this new procedure, the calculation of the liquid water content is based on the altitude above the cloud base normalized respect to the cloud thickness and the relative humidity and temperature in the cloud layer.
- Decker model: In this model proposed by Decker in [8], the function U_c has a constant value equals to either 0.9 or 0.95. For the purpose of this work, the threshold value of 0.9 was selected. In addition, an expression for w_l is also proposed, where the liquid water content into a cloud layer is assumed to be constant with height and depends only on the cloud layer thickness.

4.2. ITU-R approximate method based on local data of *L*

This model, included in Section 3.2 of the ITU-R P.840, allows estimating A_c from local measurements or estimates of *L*, in combination with cloud liquid water specific attenuation coefficient, K_l^* in dB/km/g/m^3, as seen in the following expression:

$$A_c = \frac{LK_l^*(f,273.15)}{\sin\varphi} \qquad 90° \geq \varphi \geq 5° \qquad (1)$$

where φ is the elevation angle. The value of K_l^* is calculated by:

$$K_l^*(f,T) = \frac{0.819(1.9479 \cdot 10^{-4} f^{2.308} + 2.9424 f^{0.7436} - 4.9451)}{\varepsilon''(1+\eta^2)} \tag{2}$$

The imaginary part of the complex dielectric permittivity of water vapor ε'' in (2), depends on the frequency and the temperature, as seen below:

$$\varepsilon''(f,T) = \frac{f(\varepsilon_0 - \varepsilon_1)}{f_p\left[1+(f/f_p)^2\right]} + \frac{f(\varepsilon_1 - \varepsilon_2)}{f_s\left[1+(f/f_s)^2\right]} \tag{3}$$

where:

$$\varepsilon_0 = 77.66 + 103.3(\theta - 1) \tag{4}$$

$$\varepsilon_1 = 0.0671\varepsilon_0 \tag{5}$$

$$\varepsilon_2 = 3.52 \tag{6}$$

$$\theta = 300/T \tag{7}$$

and T is the liquid water temperature in (K). The relaxation frequencies in (3), in GHz, can be calculated by the following expressions:

$$f_p = 20.20 - 146(\theta - 1) + 316(\theta - 1)^2 \tag{8}$$

$$f_s = 39.8 f_p \tag{9}$$

The parameter η is expressed as a relation between the real and imaginary part of ε, as seen below:

$$\eta = \frac{2+\varepsilon'}{\varepsilon''} \tag{10}$$

where:

$$\varepsilon'(f,T) = \frac{\varepsilon_0 - \varepsilon_1}{\left[1+(f/f_p)^2\right]} + \frac{\varepsilon_1 - \varepsilon_2}{\left[1+(f/f_s)^2\right]} + \varepsilon_2 \tag{11}$$

4.3. ITU-R approximate method based on global digital maps of L_{red}

An alternative global model has also been proposed by the ITU-R which can be used to estimate statistics of cloud attenuation at any point on Earth, in absence of either local measurements or estimates of L, as seen in Section 4.2. The model uses worldwide digital maps of annual and monthly values of L_{red}, the total columnar content of liquid water reduced to a temperature of 273.15 K, in mm. These maps are derived from the climatic reanalysis ERA-40, whose spatial resolution is 1.125° × 1.125° with a temporal resolution of 1 hour. Using this input data, annual and monthly statistics of A_c can be estimated using the following expression:

$$A_c = \frac{L_{red} K_l(f,273.15)}{\sin \varphi} \tag{12}$$

where cloud liquid water specific attenuation coefficient is given by:

$$K_l(f,T) = \frac{0.819 f}{\varepsilon''(1+\eta^2)} \tag{13}$$

5. RESULTS AND ANALYSIS

5.1. Cloud detection

Table 3 shows the results of the assessment of the 722 valid profiles using the four models described in Section 4.1. Before using the threshold function to detect the presence of clouds, profiles were classified according to the season: 301 correspond to rainy season and 421 to non-rainy season. The percentages of events where $L > 0$ mm are roughly 62.4% (Decker), 63.7% (Salonen), 53.4% (Salonen08) and 54.9% (CldMod) out of the total of radiosoundings. Although the percentages are reasonably close, differences are explained by the different formulations to calculate U_c, as well as the method to estimate w_l from one model to other Although it is true that Salonen08 and CldMod use the same U_c function which means that both models detect the same number of cloud layers, the method to calculate w_l and w_i are different, as can be verified in the references mentioned in Section 3.1. Furthermore, differences can be also

explained in the temperature value below which the presence of ice water is detected, i.e. L=0 mm, which is $-20°\text{C}$ (Salonen and Salonen08), $-30°$ C (Decker), $-35°\text{C}$ (CldMod).

TABLE 3 - NUMBER OF RADIOSOUNDINGS WITH $L > 0$ MM ESTIMATED BY DIFFERENT CLOUD DETECTION MODELS

	Number of radiosoundings		
	Rainy season	**Non-rainy season**	**Total**
Cloud Detection Model	301	421	722
Decker	250	201	451
Salonen	256	204	460
Salonen08	224	162	386
CldMod	227	170	397

Table 3 provides also some interesting information. During rainy season, the percentage of events where clouds were detected are 83% (Decker), 85% (Salonen), 74.4% (Salonen08) and 75.4% (CldMod) out of the total of radiosoundings. From a statistical point of view there would be a high probability of presence of clouds at the radiosonde launching time (12:00 UTC) between November and March. On the other hand, during the months of non-rainy season, these percentages decrease to 47.7% (Decker), 48.4% (Salonen), 38.5% (Salonen08) and 40.3% (CldMod).

5.2. Cloud attenuation

Statistics of zenith cloud attenuation are the main output of this work. Cloud effects along a slant path depend on the geometry of the link, and can be obtained by dividing the corresponding zenith values by the sine of the elevation angle, also known as the cosecant law. In propagation studies, statistics of atmospheric impairments are commonly represented as Complementary Cumulative Distribution Functions (CCDF), e.g. the amount of cloud attenuation that is exceeded a given percentage of time during a period. Due to the low temporal availability of the measurements, i.e. one radiosounding per day at 12:00 UTC, statistics have been calculated using the number of radiosondeos given in Table 3 for each cloud detection model, both taking into account the rainy and non-rainy seasons.

Figure 5 shows the CCDFs of zenith cloud attenuation calculated at 20 GHz (Ka-band), 40 GHz (Q-band) and 75 GHz (W-band) during rainy seasons. For comparison purposes, it is also included the CCDF obtained with the ITU-R global method described in Section 4.3. In order to calculate seasonal cloud attenuation with this model monthly maps were used. As seen in Figure 5, as frequency increases, from 20 GHz to 75 GHz, the absorption effects of cloud liquid water droplets become higher, thus cloud attenuation increases. At low percentages of time such as 1%, attenuation exceeds approximately 0.15 dB, 0.55 dB and 1.3 dB, respectively, using either Salonen or Salonen08. Although both models exhibit these similar values at this percentage of time, discrepancies between them are observed above 1.5% of time, being Salonen model the one with higher attenuation with respect to Salonen08. On the other hand, Decker model estimates higher cloud attenuation, reaching 0.32 dB (20 GHz), 1.05 dB (40 GHz), and 2.6 dB (75 GHz) at 1% of time, and using CldMod model, 0.45 dB (20 GHz), 1.56 dB (40 GHz), and 3.8 dB (75 GHz) are obtained. Besides, statistics based on CldMod model approach better to the ones obtained using the ITU-R global model at the three frequencies. This does not happen with Salonen model, whose statistics are quite far from ITU-R model estimates.

These previous statements have been quantitatively validated by calculating the mean value, $\bar{\varepsilon}$, and the RMS value, ε_{RMS}, of the absolute error $\varepsilon(p)$ given by (14), where p is the percentage of time:

$$\varepsilon(p) = A_{c,ITU}(p) - A_{c,model}(p) \tag{14}$$

The results are shown in Tables 4 to 6. The lower error metrics are those obtained using CldMod model, next those of Decker model. These results are striking because, since the publication of the CldMod model, its use has not been usually reported in propagation studies. However, it is worth mentioning that the accuracy of digital maps at very high altitude sites should be assessed and could be at the origin of unexpected results. On the other hand, Tables 4 to 6 confirm that the worst error metrics are obtained with Salonen and Salonen08 models.
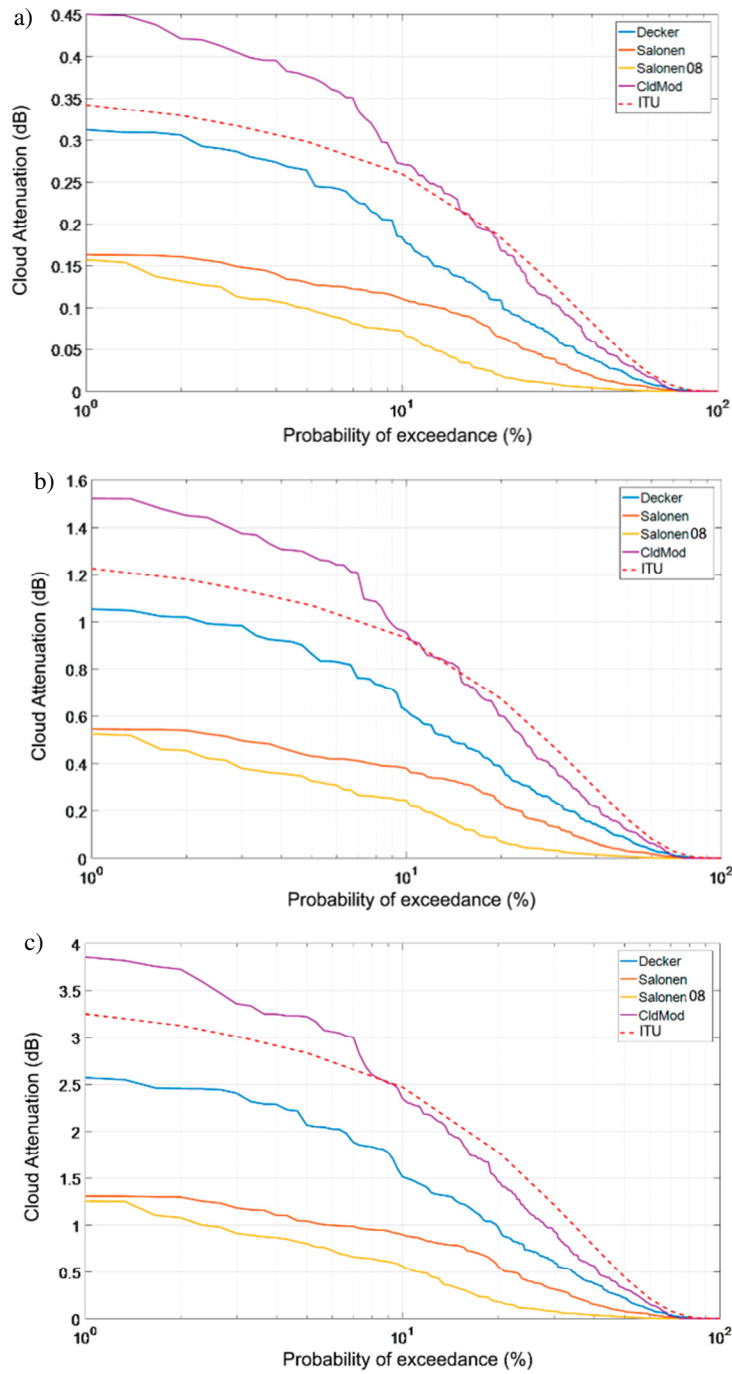
Figure 5: CCDFs of zenith cloud attenuation during rainy season (2016-2019) by the ITU-R model based on L values and different cloud detection models (solid lines), and by approximate ITU-R model based on data of ERA-40 (dashed line) for a) 20 GHz, b) 40 GHz and c) 75 GHz.

TABLE 4 - MEAN AND RMS VALUES OF THE ABSOLUTE ERROR BETWEEN $A_{c\ UIT}$ *and* $A_{c\ model}$ AT 20 GHZ IN RAINY SEASON

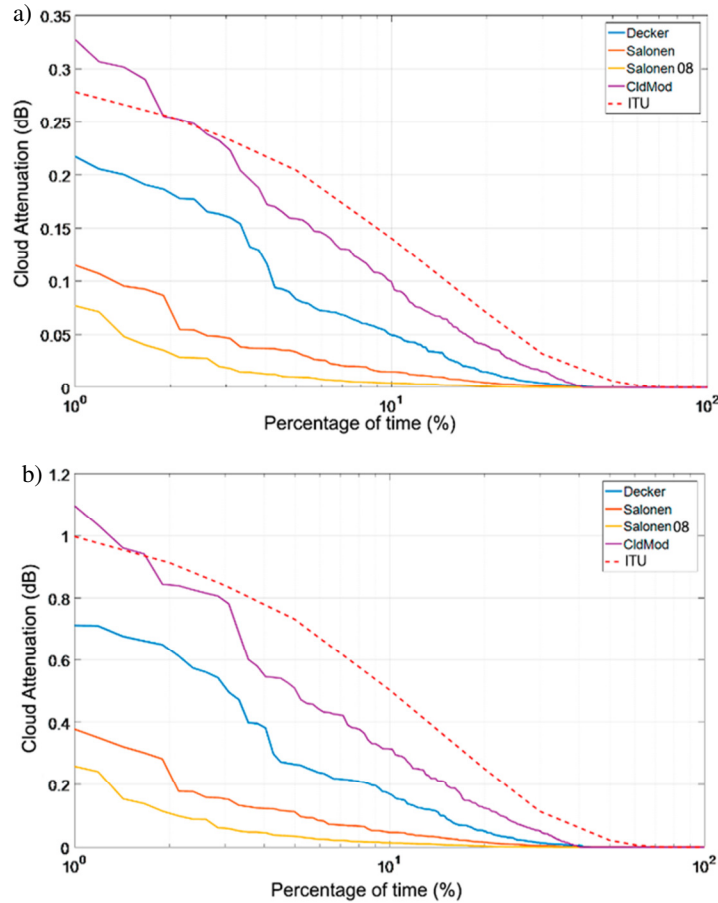| Error metric (dB)	Cloud Detection Model			
	Decker	Salonen	Salonen08	CldMod
$\bar{\varepsilon}$	0.027	0.079	0.095	**-0.023**
ε_{RMS}	0.027	0.074	0.087	**0.044**

TABLE 5 - MEAN AND RMS VALUES OF THE ABSOLUTE ERROR BETWEEN $A_{c\,UIT}$ and $A_{c\,model}$ AT 40 GHZ IN RAINY SEASON

Error metric (dB)	Cloud Detection Model			
	Decker	Salonen	Salonen08	CldMod
$\bar{\varepsilon}$	0.119	0.297	0.351	**-0.056**
ε_{RMS}	0.142	0.354	0.413	**0.134**

TABLE 6 - MEAN AND RMS VALUES OF THE ABSOLUTE ERROR BETWEEN $A_{c\,UIT}$ and $A_{c\,model}$ AT 75 GHZ IN RAINY SEASON

Error metric (dB)	Cloud Detection Model			
	Decker	Salonen	Salonen08	CldMod
$\bar{\varepsilon}$	0.392	0.836	0.968	**-0.069**
ε_{RMS}	0.506	1.097	1.254	**0.289**

To conclude, Figure 7 shows the CCDFs of zenith cloud attenuation calculated at the three selected frequencies during non-rainy seasons, using the four cloud detection models. Similarly, as shown previously, the CCDF obtained using ITU-R global model is also included for the sake of comparison. Cloud attenuation statistics exceeded 1% of time, during non-rainy periods; vary between 0.08 and 0.33 dB (20 GHz), 0.26 and 1.1 dB (40 GHz), and 0.62 and 2.6 dB (75 GHz) in function of the cloud detection model. As it can be seen, the ITU-R estimates higher attenuation values with respect to those given by cloud detection models. Notwithstanding this fact, CldMod is still close to the ITU-R results as it was seen in the previous analysis for rainy season. In addition, Tables 7 to 9 summarize the results of the error analysis confirming that cloud attenuation statistics using CldMod has the lower values of $\bar{\varepsilon}$ and ε_{RMS} when compared to ITU-R global model.
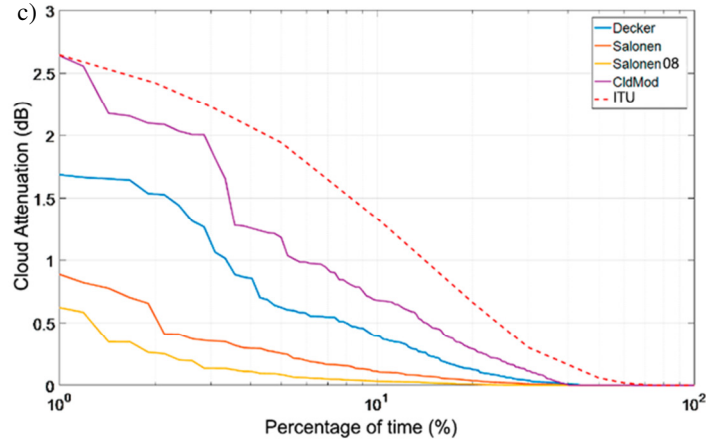
Figure 6: Total CCDFs for the non-rainy season of A_c values in zenith estimated by the ITU-R model based on L values and different cloud detection models (solid lines), and by approximate ITU-R model based on data of ERA-40 (dashed line) for a) 20 GHz, b) 40 GHz and c) 75 GHz.

TABLE 7 - MEAN AND RMS VALUES OF THE ABSOLUTE ERROR BETWEEN $A_{c\,UIT}$ and $A_{c\,model}$ AT 20 GHZ IN THE NON-RAINY SEASON

	Cloud Detection Model			
Error metric (dB)	Decker	Salonen	Salonen08	CldMod
$\bar{\varepsilon}$	0.036	0.067	0.077	**0.007**
ε_{RMS}	0.041	0.078	0.093	**0.038**

TABLE 8 - MEAN AND RMS VALUES OF THE ABSOLUTE ERROR BETWEEN $A_{c\,UIT}$ and $A_{c\,model}$ AT 40 GHZ IN NON-RAINY SEASON

	Cloud Detection Model			
Error metric (dB)	Decker	Salonen	Salonen08	CldMod
$\bar{\varepsilon}$	0.144	0.245	0.279	**0.047**
ε_{RMS}	0.198	0.329	0.377	**0.108**

TABLE 9 - MEAN AND RMS VALUES OF THE ABSOLUTE ERROR BETWEEN $A_{c\,UIT}$ and $A_{c\,model}$ AT 75 GHZ IN NON-RAINY SEASON

	Cloud Detection Model			
Error metric (dB)	Decker	Salonen	Salonen08	CldMod
$\bar{\varepsilon}$	0.434	0.672	0.748	**0.195**
ε_{RMS}	0.630	0.982	1.100	**0.333**

6. CONCLUSIONS

Measuring cloud attenuation by experimental means using specialized instruments is neither an easy nor a usual task in slant-path propagation experiments. In the present work, a technique has been used to estimate statistics of cloud attenuation at 20, 40 and 75 GHz using vertical meteorological profiles collected in Bolivia at 4065 meters above mean sea level. To our knowledge, few studies have been published worldwide under such geographical conditions.

Four different models have been implemented to perform this estimation, which in addition, has been carried out by considering rainy and non-rainy seasons. The results have been compared to the statistics given by the most recent version of the ITU-R cloud attenuation global model. As seen, cloud attenuation increases with frequency, which confirms the increasing that cloud bodies will have in future satellite communication systems, in Q and W band. In Ka band, the effect is less relevant. In rainy season the probability of presence of clouds is high, including precipitating

clouds which likely have important amount of liquid water content, thus, attenuation cause by clouds in this period is higher than in non-rainy season.

An unexpected observation is that the CldMod model provides statistics which are closer to the ones obtained by the ITU-R global model. The Decker model presents bit more discrepancies, and Salonen and Salonen08 are quite far from the model recommended by the ITU-R. To date, CldMod model has been hardly used by propagation experimenters in similar studies using radiosoundings. However, this conclusion has to be carefully analyzed. The reader has to be aware that this result is a comparison of estimation models. Although the use of the ITU-R global model is recommended for using worldwide, it is based on digital maps extracted from ERA-40 NWP. The accuracy of the meteorological parameters found in that database, for high altitude sites, should be carefully assessed because could be at the origin of the results obtained in this study.

To conclude, we believe that future works should continue assessing atmospheric propagation conditions in high altitude sites. In absence of connectivity in several towns and villages located in Andean regions in Latin America, satellite communications are still a viable solution, therefore, the understanding and characterization of propagation phenomena have to be improved.

ACKNOWLEDGMENTS

REFERENCES

[1] T. Rossi et al., "Satellite communication and propagation experiments through the Alphasat Q/V band Aldo Paraboni technology demonstration payload," in *IEEE Aerospace and Electronic Systems Magazine*, vol. 31, no. 3, pp. 18-27, March 2016.

[2] S. De Fina, M. Ruggieri and A. V. Bosisio, "Exploitation of the W-band for high capacity satellite communications," in *IEEE Transactions on Aerospace and Electronic Systems*, vol. 39, no. 1, pp. 82-93, Jan. 2003.

[3] G. A. Siles, M. Heredia and R. Harriague, "Cloud detection models and their effect on the calculation of cloud attenuation: Assessment at Ka-and Q-band at 4065 meters of altitude,"*14th European Conference on Antennas and Propagation (EuCAP)*, 2020, pp. 1-5.

[4] ITU-R, "Attenuation due to clouds and fogs," *ITU-R Recommendation P.840-8*, 2019

[5] M. F. Andrade, I. Moreno, J.M. Calle, L. Ticona, L. Blacutt, W. Lavado-Casimiro, E. Sabino, A. Huerta, C. Aybar, S. Hunziker, S. Brönnimann, *Climate and extreme events from the Central Altiplano of Peru and Bolivia 1981-2010*. Geographica Bernensia. 2018.

[6] E. Salonen and S. Uppala, "New prediction method of cloud attenuation," *Electronics Letters*, vol. 27, no. 12, pp. 1106–1108, 1991.

[7] V. Mattioli, P. Basili, S. Bonafoni, P. Ciotti, and E. Westwater, "Analysis and improvements of cloud models for propagation studies," *Radio Science*, vol. 44, 2009.

[8] M. Decker, E. Westwater, and F. Guiraud, "Experimental evaluation of ground-based microwave radiometric sensing of atmospheric temperature and water vapor profiles," *Journal of Applied Meteorology*, vol. 17, no. 12, pp. 1788–1795, 1978.